EEG spectro-temporal amplitude modulation as a measurement of cortical hemodynamics: an EEG-fNIRS study

Lucas R. Trambaiolli[1], Raymundo Cassani[2] and Tiago H. Falk[2]

***Abstract*— Neurovascular coupling provides valuable descriptive information about neural function and communication. In this work, we propose to objectively characterize EEG sub-band modulation in an attempt to compare with local variations of fNIRS hemoglobin concentration. First, full-band EEG signals are decomposed into five well-known frequency sub-bands: delta, theta, alpha, beta, and gamma. The temporal amplitude envelope of each sub-band is then computed via Hilbert transformation. The proposed EEG 'spectro-temporal amplitude modulation' (EEG-AM) feature measures the rate at which each sub-band is modulated. Similarities between EEG-AM features and fNIRS hemoglobin concentration are computed for four neighboring channels over the occipital area during resting-state. Experiments with a database of 29 participants show statistically significant similarities between the total hemoglobin concentration and the alpha band modulating the alpha, beta, and gamma frequencies. These results support the idea that the EEG-AM can carry hemodynamic properties.**

***Clinical relevance*— This shows that the EEG spectro-temporal amplitude modulation present similarities with the hemoglobin concentration in co-placed channels.**

I. INTRODUCTION

Given the limited intra-cellular capacity for energy storage, local neural, or associated support cells, neural activity leads to local changes in blood flow to supply its metabolic demand [1]. This phenomenon is named neurovascular coupling, and was widely studied in both humans and animals. For example, simultaneous functional magnetic resonance imaging (fMRI) and local field potential records in monkeys revealed correlated spontaneous fluctuations over the cortex between the blood oxygen level-dependent (BOLD) signals and the gamma-band power [2]. In humans, the fMRI-BOLD signal is continuously related to electroencephalographic (EEG) oscillations, for example, presenting an inverse correlation between the BOLD signal amplitude and the alpha-band power [3].

In this context, there is a growing interest in identifying EEG features capable of describing hemodynamic alterations in the human brain. Of particular interest is the evaluation of the EEG spectro-temporal amplitude-modulation (AM) as a representation of synchronized interactions of neural and metabolic systems [4], [5]. Indeed, previous studies have shown a linear correlation between local EEG-AM and gray-matter blood flow [6], [7]. Also, EEG-AM has been used to predict the performance of an hemodynamic-based neurofeedback task [8], and to classify patients with Alzheimer's disease [9], [10] (a neurological disorder known for presenting reduced cerebral blood flow [11]).

One relevant tool to investigate neuro-electric and neuro-hemodynamic relations is the use of simultaneous EEG and functional near-infrared spectroscopy (fNIRS), since these methods do not present electro-optical interference, allowing the investigation of gray matter neurovascular coupling [12]. Also, although not perfectly spatiotemporally correspondent, source estimation of EEG and fNIRS signals showed a significant level of corresponding sensitivity to gray matter activity between co-localized channels [13]. At the same time, the EEG-AM presented coupling with fNIRS hemoglobin measurements [14].

In this paper, we evaluated which EEG-AM bands present similar signal properties with fNIRS total hemoglobin concentrations. In a population of 29 healthy subjects, our results suggest that the alpha modulation band present oscillations similar to the hemodynamic function.

II. METHODS

A. Database

Herein, we used a publicly available dataset [15] composed by simultaneous EEG-fNIRS recordings from 29 healthy participants (28.41 ± 3.75 years, 16 females). For each subject, data were recorded from 30 EEG channels using a BrainAmp EEG amplifier (Brain Products GmbH, Germany) with linked mastoids reference at 1000 Hz sampling rate, and from 14 fNIRS sources and 16 fNIRS detectors recorded by NIRScout equipment (NIRx GmbH, Germany) at 12.5 Hz sampling rate. Four different experimental conditions are available, including motor imagery of each hand, mental arithmetic, and resting-state, with 30 trials per condition.

For this study, we focused on two EEG and three fNIRS channels situated over the occipital/visual cortex (Figure 1) during resting-state trials with eyes open. These channels were selected as the occipital/visual cortex is less susceptible to biological artifacts such as electrooculography (EOG) and electromyography (EMG) [16]. Moreover, it is widely used in animal and human studies of neurovascular coupling [17]. Both EEG and fNIRS signals were segmented into 30 epochs of 22 s, that include 2 s of instruction, 10 s of resting-state "task" and an additional 10 s of inter-trial rest, according to the original paper [15].

[1]L.R. Trambaiolli is with the McLean Hospital, Harvard Medical School, Belmont, USA ltrambaiolli@mclean.harvard.edu

[2]R. Cassani and T.H. Falk are with the Institut national de la recherche scientifique (INRS-EMT), University of Quebec, Montreal, Canada raymundo.cassani@emt.inrs.ca, falk@emt.inrs.ca

978-1-7281-1990-8/20/$31.00 ©2020 IEEE

Authorized licensed use limited to: Harvard Library. Downloaded on June 13,2023 at 03:10:13 UTC from IEEE Xplore. Restrictions apply.

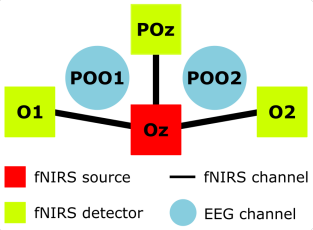

Fig. 1. Configuration of the occipital channels [15]. Blue circles: EEG channels; Red squares: fNIRS sources; Green squares: fNIRS detectors; Black lines: fNIRS channels.

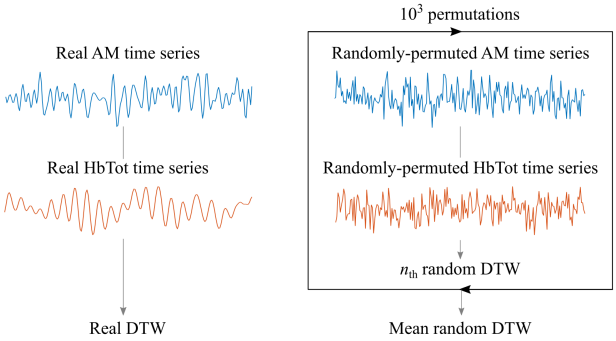

Fig. 2. DTW computation performed in each epoch.

B. EEG preprocessing

First, each channel was band-pass filtered between 0.1-45 Hz by zero-phase finite impulse response (FIR) filter. Then, EEG amplitude modulations (EEG-AM) [10] were computed for each channel. For this, temporal series were decomposed into five classic spectral bands: delta (0.1-4.0 Hz), theta (4.0-8.0 Hz), alpha (8.0-12.0 Hz), beta (12.0-30.0 Hz) and gamma (30.0-45.0 Hz). For each band, the temporal envelope was extracted using the Hilbert transform. Then, each envelope was decomposed into five modulation bands, named: m-delta (0.1-4.0 Hz), m-theta (4.0-8.0 Hz), m-alpha (8.0-12.0 Hz), m-beta (12.0-30.0 Hz) and m-gamma (30.0-45.0 Hz). All decompositions were carried on with FIR filters as they possess linear phase. However, due to Bedrosian's theorem [18], the envelope signal can only contain modulation frequencies up to the maximum frequency of its originating signal. Hence, if we use the notation "frequency band - m - modulation band", only the following EEG-AM are relevant: delta-m-delta, theta-m-delta, theta-m-theta, alpha-m-delta, alpha-m-theta, alpha-m-alpha, beta-m-delta, beta-m-theta, beta-m-alpha, beta-m-beta, gamma-m-delta, gamma-m-theta, gamma-m-alpha, gamma-m-beta and gamma-m-gamma. Finally, each time series was down-sampled to the sampling rate of the fNIRS signals.

C. fNIRS preprocessing

The fNIRS data were preprocessed using the HOMER2 toolbox [19]. First, temporal series were detrended by their respective whole-length record (without segmentation). The total hemoglobin (HbTot) concentration was computed using the modified Beer-Lambert law [20], with the dynamic path factors (DPF) set 6.25 and 5.19 for the lower and higher wavelengths, respectively. These DPF values were calculated based on the average age of the sample [21]. Next, the time series was band-filtered between 0.1 and 1.0 Hz by a phase linear filter to remove artifacts due to heartbeat, respiration, and Mayer waves.

D. Dynamic time warping

We used the dynamic time warping (DTW) algorithm [22] to compare the EEG-AM and fNIRS-HbTot time series. Since EEG-AM and HbTot present different measurement units, each signal was normalized to have zero mean, and standard-deviation equal to one. We conducted four comparisons between neighboring channels: "POO1 (EEG) $\times$ Oz-POz (fNIRS)", "POO1 (EEG) $\times$ Oz-O1 (fNIRS)", "POO2 (EEG) $\times$ Oz-POz (fNIRS)", and "POO2 (EEG) $\times$ Oz-O2 (fNIRS)".

For each resting-state epoch, we first computed the DTW between each AM-HbTot pair. Then, we randomly permuted samples in each time series and calculated the DTW value between these "random" signals. The permutation process was repeated 10^3 times, and the resulting values were averaged in each epoch. This process is illustrated in Figure 2. Later, the DTW values were averaged across epochs to product one single real DTW and one random DTW value per subject. We used a single-tailed t-test to evaluate if the DTW values from the original time series were smaller than the random DTW values across subjects. False-discovery-rate correction was used on the resulting p-values for 60 multiple comparisons (4 EEG-fNIRS pairs $\times$ 15 AM-HbTot pairs).

III. RESULTS

Table I presents the differences (mean $\pm$ standard-deviation) between real DTW values and random DTW values for each EEG-fNIRS pair (columns), and each AM-HbTot pair (lines). Bold items represent the comparisons where the real DTW values were significantly smaller than the random ones (p-value$<$0.01).

As can be seen, all alpha modulations (alpha-m-alpha, beta-m-alpha, and gamma-m-alpha) present significant DTW differences for all pairs of channels, indicating that the coupling between these signals is consistent over the occipital cortex. To further illustrate the coupling between signals, Figure 3 shows the averaged EEG signals (in blue) for each of the significant amplitude modulations (alpha-m-alpha, beta-m-alpha, and gamma-m-alpha) and fNIRS HbTot (in red) for one subject, in two pairs of channels. As can be seen, although the fNIRS time series present a delayed beginning of oscillations with a higher amplitude, all pairs of channels show several moments of overlapping cycles starting around five seconds.

IV. DISCUSSION

A. Alpha frequencies and neurovascular coupling

The significant similarity between alpha modulation features and the total hemoglobin concentration is somehow expected, as alpha frequencies are a known signature of

Authorized licensed use limited to: Harvard Library. Downloaded on June 13,2023 at 03:10:13 UTC from IEEE Xplore. Restrictions apply.

TABLE I

AVERAGE DIFFERENCES BETWEEN THE DTW (ΔDTW) COMPARING REAL SIGNALS AND RANDOMLY-PERMUTED SIGNALS.

EEG-AM	POO1 (EEG) x Oz-POz (fNIRS)		POO1 (EEG) x Oz-O1 (fNIRS)		POO2 (EEG) x Oz-POz (fNIRS)		POO2 (EEG) x Oz-O2 (fNIRS)	
	ΔDTW	p-value	ΔDTW	p-value	ΔDTW	p-value	ΔDTW	p-value
delta-m-delta	15.88±12.65	1.00	15.01±9.07	1.00	15.67±12.52	1.00	16.89±12.99	1.00
theta-m-delta	25.01±9.46	1.00	24.26±7.05	1.00	24.96±9.77	1.00	26.02±10.44	1.00
theta-m-theta	42.65±2.15	1.00	42.31±1.63	1.00	42.67±1.97	1.00	42.81±2.08	1.00
alpha-m-delta	19.12±11.11	1.00	18.64±8.82	1.00	19.29±11.22	1.00	20.35±11.64	1.00
alpha-m-theta	39.90±3.20	1.00	39.89±2.94	1.00	39.84±3.22	1.00	40.08±3.44	1.00
alpha-m-alpha	**-17.66±5.96**	**<0.01**	**-18.80±5.31**	**<0.01**	**-17.35±6.24**	**<0.01**	**-16.32±6.37**	**<0.01**
beta-m-delta	26.96±9.12	1.00	26.33±7.41	1.00	26.90±9.37	1.00	27.52±9.58	1.00
beta-m-theta	45.14±4.33	1.00	44.66±3.65	1.00	45.20±4.49	1.00	45.40±4.57	1.00
beta-m-alpha	**-14.44±9.74**	**<0.01**	**-16.15±8.19**	**<0.01**	**-14.44±9.98**	**<0.01**	**-13.10±10.54**	**<0.01**
beta-m-beta	36.66±4.95	1.00	36.14±3.79	1.00	36.59±4.74	1.00	36.98±4.74	1.00
gamma-m-delta	29.30±9.18	1.00	28.86±7.65	1.00	29.18±9.35	1.00	29.74±9.28	1.00
gamma-m-theta	45.02±5.34	1.00	44.67±4.66	1.00	45.22±5.54	1.00	45.21±5.67	1.00
gamma-m-alpha	**-13.96±10.45**	**<0.01**	**-15.50±7.88**	**<0.01**	**-14.03±10.60**	**<0.01**	**-13.01±11.00**	**<0.01**
gamma-m-beta	32.21±5.56	1.00	31.87±4.86	1.00	32.01±5.69	1.00	32.47±5.61	1.00
gamma-m-gamma	2.55±4.20	1.00	2.43±3.82	1.00	2.27±4.50	1.00	2.71±4.23	1.00

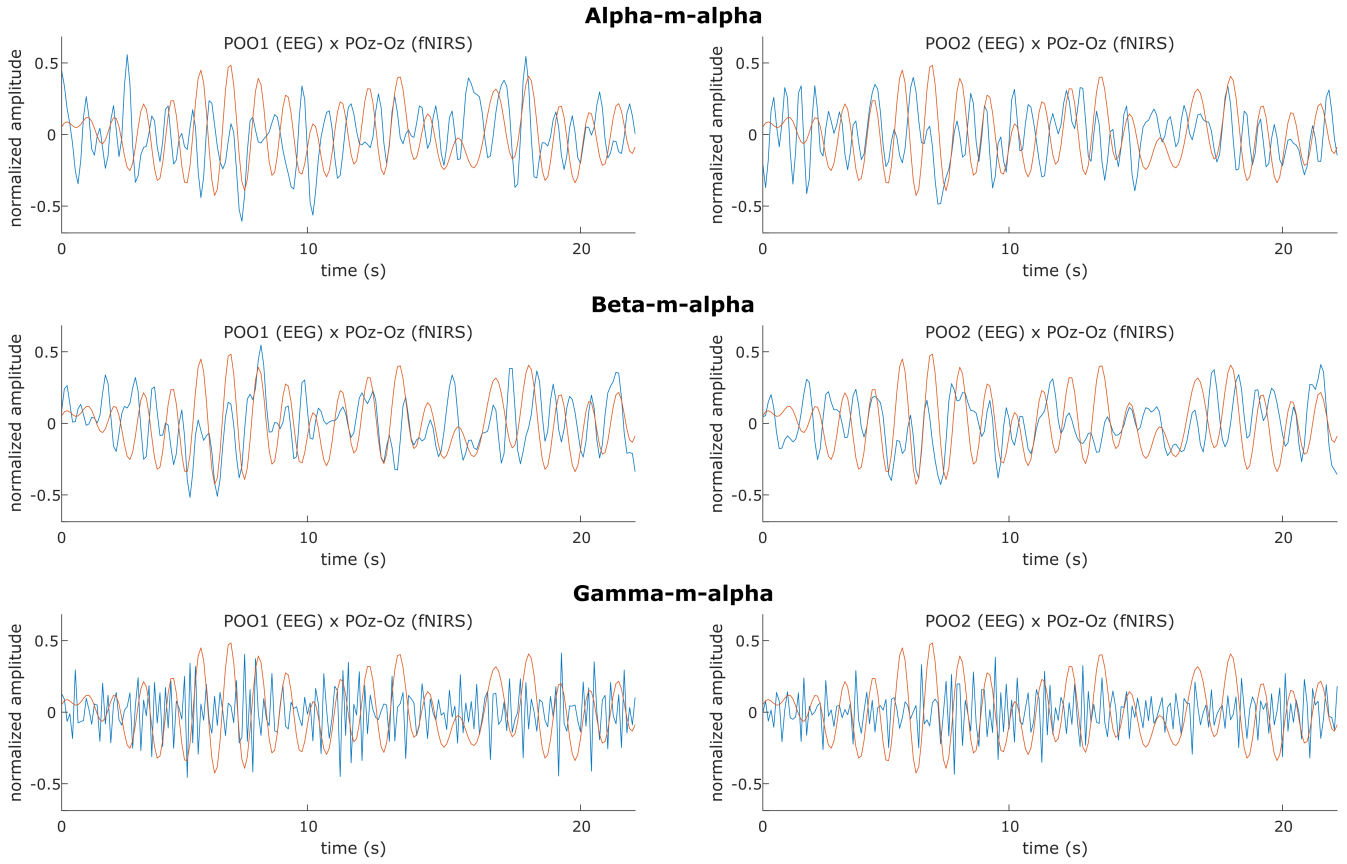

Fig. 3. Average EEG alpha modulations (blue) and fNIRS total hemoglobin (red) from one subject.

resting-state and, consequently, a biomarker of cognitive workload or relaxation. For example, it is related with variations in heart rate [23], and brain connectivity [24].

Previous studies using EEG-PET recordings show a positive correlation between the average blood concentration and the average values of the alpha modulation [6], [7]. Later, fMRI-EEG experiments reported the existence of BOLD oscillations similar to the EEG alpha frequency [25]. Alpha frequencies were also able to predict fNIRS blood oxygenation in different areas across the scalp [26], [27].

Another expected fact is the temporal shift between the EEG and fNIRS oscillations. Neurons do not rely upon the blood flow to meet their initial metabolic needs, given their local storage of oxygen and glucose to supply the immediate demands [28]. Once the initial supplies are depleted, an increased blood flow is needed to replenish supplies or to sustain prolonged neuronal responses [1].

B. Significance

Having an EEG feature correlated with hemodynamic function opens the window for new sets of investigations

Authorized licensed use limited to: Harvard Library. Downloaded on June 13,2023 at 03:10:13 UTC from IEEE Xplore. Restrictions apply.

where an fMRI setup is not accessible [29]. For example, when evaluating cortical blood-flow impairment in clinical populations far from the great fMRI centers. When combined with fNIRS recordings, it is possible to evaluate neurovascular coupling during naturalistic tasks [30].

C. Limitations and ongoing investigations

Depending on the fNIRS setup, it may also encompass peripheral responses, including changes in non-neuronal blood flow (e.g., from skin or muscular surfaces). One approach that should be adopted in future studies is the use of short-distance channels to filter systemic hemodynamic fluctuations from non-neural sources [31]. Also, this study is limited to the evaluation of occipital channels during resting state trials. Future studies will evaluate the consistency of the results in different scalp regions during different tasks.

V. CONCLUSIONS

In this work, the relationship between EEG features and local hemodynamics is demonstrated. The feature, termed "spectro-temporal amplitude modulation," measures the rate with which EEG sub-band signals are modulated. Experiments with a simultaneous EEG-fNIRS database measured from 29 participants show that EEG alpha modulations present similar temporal patterns to total hemoglobin concentration measured with fNIRS. This feature has the potential to assist researchers interested in evaluating correspondences between EEG and hemodynamic activity. As EEG and fNIRS are potentially portable techniques, the results herein presented an opportunity to perform neurovascular coupling experiments in more natural situations.

REFERENCES

[1] A. A. Phillips, F. H. Chan, M. M. Z. Zheng, A. V. Krassioukov, and P. N. Ainslie, "Neurovascular coupling in humans: physiology, methodological advances and clinical implications," *J. Cereb. Blood Flow Metab.*, vol. 36, no. 4, pp. 647–664, 2016.

[2] M. L. Schölvinck, A. Maier, Q. Y. Frank, J. H. Duyn, and D. A. Leopold, "Neural basis of global resting-state fMRI activity," *Proc. Natl. Acad. Sci. U.S.A.*, vol. 107, no. 22, pp. 10 238–10 243, 2010.

[3] R. I. Goldman, J. M. Stern, J. Engel Jr, and M. S. Cohen, "Simultaneous EEG and fMRI of the alpha rhythm," *Neuroreport*, vol. 13, no. 18, p. 2487, 2002.

[4] P. Novak, V. Lepicovska, and C. Dostalek, "Periodic amplitude modulation of EEG," *Neurosci. Lett.*, vol. 136, no. 2, pp. 213–215, 1992.

[5] A. Bondar and A. Fedotchev, "Concerning the amplitude modulation of the human EEG," *Hum. Physiol.*, vol. 26, no. 4, pp. 393–399, 2000.

[6] D. Ingvar, I. Rosen, and G. Johannesson, "EEG related to cerebral metabolism and blood flow," *Pharmacopsychiatry*, vol. 12, no. 02, pp. 200–209, 1979.

[7] J. G. Okyere, P. Y. Ktonas, and J. S. Meyer, "Quantification of the alpha EEG modulation and its relation to cerebral blood flow," *IEEE Trans. Biomed. Eng.*, no. 7, pp. 690–696, 1986.

[8] L. Trambaiolli, R. Cassani, C. Biazoli, A. Cravo, J. Sato, and T. Falk, "Resting-awake EEG amplitude modulation can predict performance of an fNIRS-based neurofeedback task," in *2018 International Conference on Systems, Man, and Cybernetics*. IEEE, 2018, pp. 1128–1132.

[9] L. R. Trambaiolli, T. H. Falk, F. J. Fraga, R. Anghinah, and A. C. Lorena, "EEG spectro-temporal modulation energy: a new feature for automated diagnosis of Alzheimer's disease," in *2011 Annual International Conference of the Engineering in Medicine and Biology Society*. IEEE, 2011, pp. 3828–3831.

[10] T. H. Falk, F. J. Fraga, L. Trambaiolli, and R. Anghinah, "EEG amplitude modulation analysis for semi-automated diagnosis of Alzheimer's disease," *EURASIP J. Adv. Signal Process.*, vol. 2012, no. 1, p. 192, 2012.

[11] K. Kisler, A. R. Nelson, A. Montagne, and B. V. Zlokovic, "Cerebral blood flow regulation and neurovascular dysfunction in Alzheimer's disease," *Nat. Rev. Neurosci.*, vol. 18, no. 7, p. 419, 2017.

[12] A. M. Chiarelli, F. Zappasodi, F. Di Pompeo, and A. Merla, "Simultaneous functional near-infrared spectroscopy and electroencephalography for monitoring of human brain activity and oxygenation: a review," *Neurophotonics*, vol. 4, no. 4, p. 041411, 2017.

[13] P. Giacometti and S. G. Diamond, "Correspondence of electroencephalography and near-infrared spectroscopy sensitivities to the cerebral cortex using a high-density layout," *Neurophotonics*, vol. 1, no. 2, p. 025001, 2014.

[14] M. T. Talukdar, H. R. Frost, and S. G. Diamond, "Modeling neurovascular coupling from clustered parameter sets for multimodal EEG-NIRS," *Comput. Math. Methods Med.*, vol. 2015, 2015.

[15] J. Shin, A. von Lühmann, B. Blankertz, D.-W. Kim, J. Jeong, H.-J. Hwang, and K.-R. Müller, "Open access dataset for EEG+NIRS single-trial classification," *IEEE Trans. Neural Syst. Rehabil. Eng.*, vol. 25, no. 10, pp. 1735–1745, 2016.

[16] R. Anghinah, L. I. Basile, M. T. Schmidt, K. Sameshima, and W. F. Gattaz, "Biologic artifacts in quantitative EEG," *Arq. Neuropsiquiatr.*, vol. 64, no. 2A, pp. 264–268, 2006.

[17] Y.-R. Gao, Y. Ma, Q. Zhang, A. T. Winder, Z. Liang, L. Antinori, P. J. Drew, and N. Zhang, "Time to wake up: Studying neurovascular coupling and brain-wide circuit function in the un-anesthetized animal," *Neuroimage*, vol. 153, pp. 382–398, 2017.

[18] E. Bedrosian, "A product theorem for Hilbert transforms," *Proc. IEEE*, vol. 51, no. 5, pp. 868–869, 1963.

[19] T. J. Huppert, S. G. Diamond, M. A. Franceschini, and D. A. Boas, "HomER: a review of time-series analysis methods for near-infrared spectroscopy of the brain," *Appl. Opt.*, vol. 48, no. 10, pp. D280–D298, 2009.

[20] D. T. Delpy, M. Cope, P. van der Zee, S. Arridge, S. Wray, and J. Wyatt, "Estimation of optical pathlength through tissue from direct time of flight measurement," *Phys. Med. Biol.*, vol. 33, no. 12, p. 1433, 1988.

[21] F. Scholkmann and M. Wolf, "General equation for the differential pathlength factor of the frontal human head depending on wavelength and age," *J. Biomed. Opt.*, vol. 18, no. 10, p. 105004, 2013.

[22] D. J. Berndt and J. Clifford, "Using dynamic time warping to find patterns in time series." in *Knowledge Discovery in Data Workshop*, vol. 10, no. 16. Seattle, WA, 1994, pp. 359–370.

[23] J. C. de Munck, S. I. Gonçalves, T. J. Faes, J. P. Kuijer, P. J. Pouwels, R. M. Heethaar, and F. L. da Silva, "A study of the brain's resting state based on alpha band power, heart rate and fMRI," *Neuroimage*, vol. 42, no. 1, pp. 112–121, 2008.

[24] R. Scheeringa, K. M. Petersson, A. Kleinschmidt, O. Jensen, and M. C. Bastiaansen, "EEG alpha power modulation of fMRI resting-state connectivity," *Brain Connect.*, vol. 2, no. 5, pp. 254–264, 2012.

[25] L. Wu, T. Eichele, and V. D. Calhoun, "Reactivity of hemodynamic responses and functional connectivity to different states of alpha synchrony: a concurrent EEG-fMRI study," *Neuroimage*, vol. 52, no. 4, pp. 1252–1260, 2010.

[26] G. Pfurtscheller, I. Daly, G. Bauernfeind, and G. R. Müller-Putz, "Coupling between intrinsic prefrontal HbO2 and central EEG beta power oscillations in the resting brain," *PLoS ONE*, vol. 7, no. 8, p. e43640, 2012.

[27] P. Lachert, D. Janusek, P. Pulawski, A. Liebert, D. Milej, and K. J. Blinowska, "Coupling of Oxy-and Deoxyhemoglobin concentrations with EEG rhythms during motor task," *Sci. Rep.*, vol. 7, no. 1, p. 15414, 2017.

[28] E. M. Hillman, "Coupling mechanism and significance of the BOLD signal: a status report," *Annu. Rev. Neurosci.*, vol. 37, pp. 161–181, 2014.

[29] R. Cassani, T. H. Falk, F. J. Fraga, M. Cecchi, D. K. Moore, and R. Anghinah, "Towards automated electroencephalography-based alzheimer's disease diagnosis using portable low-density devices," *Biomed. Signal. Process. Control*, vol. 33, pp. 261–271, 2017.

[30] J. B. Balardin, G. A. Zimeo Morais, R. A. Furucho, L. Trambaiolli, P. Vanzella, C. Biazoli Jr, and J. R. Sato, "Imaging brain function with functional near-infrared spectroscopy in unconstrained environments," *Front. Hum. Neurosci.*, vol. 11, p. 258, 2017.

[31] S. Brigadoi and R. J. Cooper, "How short is short? optimum source–detector distance for short-separation channels in functional near-infrared spectroscopy," *Neurophotonics*, vol. 2, no. 2, p. 025005, 2015.

Authorized licensed use limited to: Harvard Library. Downloaded on June 13,2023 at 03:10:13 UTC from IEEE Xplore. Restrictions apply.